

# Effective Field Theory for Atom-Molecule Systems

## I: Formulation of Effective Field Theory

Catarina E Sahlberg and C W Gardiner

*Jack Dodd Centre for Quantum Technology,  
Department of Physics, University of Otago,  
Dunedin, New Zealand*

August 29, 2018

### Abstract

We present a model of a coupled bosonic atom-molecule system, using the recently developed c-field methods as the basis in our formalism. We derive expressions for the s-wave scattering length and binding energy within this formalism, and by relating these to the corresponding experimental parameters, we can accurately determine the phenomenological parameters in our system.

## 1 Introduction

C-field methods have become an indispensable tool in the quantitative description of many aspects of Bose–Einstein condensation physics [1], providing a description of the dynamics of highly degenerate Bosonic gases, which incorporates quantum mechanics correctly, and is accurate provided the density of the Bose gas is sufficiently high.

The c-field method is based on the use of a Wigner function representation, in which a truncation approximation is made, and this is valid when the density of the Bose–Einstein condensate is large—for details the reader is referred to [1]. The mathematical formulation of the c-field method which results from this is superficially very similar to that provided by the Gross–Pitaevskii equation. The principal feature in addition to the Gross–Pitaevskii equation is provided by the inclusion of a stochastic representation of quantum fluctuations in the initial conditions. In the high density limit the method provides a treatment in which quantum and thermal phenomena are correctly accounted for. The predictions of c-field calculations can be dramatically different from those of the Gross–Pitaevskii equation, as was shown in the treatment of colliding condensates [2–4], in which the c-field method was first introduced.

The quantum fluctuations correspond to half a quantum of noise added to each degree of freedom; to avoid ultraviolet divergence it is therefore necessary to restrict the number of modes used. In practice this is done by means of a projection of the equations of motion into a subspace with a maximum momentum, usually called  $\hbar\Lambda$ . Such a cutoff is necessary for two other reasons:

1. Numerical computations must always be restricted to a finite number of modes. This is most commonly provided by the spatial grid, although, as shown in [1], this must be implemented as a projector into the relevant mode subspace if aliasing is to be avoided. This issue is not so important for simple Gross–Pitaevskii equation

simulations, since the occupations of modes at risk of being aliased are usually small, but the in the c-field method *every* mode has at least a half quantum of occupation, and aliasing is definitely an issue of concern.

2. As in the Gross-Pitaevskii equation, the interactions between the condensed particles in the c-field formalism are represented by a localized contact potential. This pseudopotential method implies the use of a cutoff, as has been argued by Braaten and Nieto [5], who introduced the requirement on the cutoff  $\Lambda$  and the interparticle scattering length  $a_s$

$$\Lambda a_s \ll 1, \tag{1}$$

for the validity of a pseudopotential method.

As implied by our use of the same notation  $\Lambda$ , the pseudopotential cutoff and that required by the numerical simulations are in practice essentially identical. (In principle there is a difference, discussed in the appendix.) In practice the choice of cutoff mandated by the numerical algorithms used satisfies this criterion with a satisfactory margin of safety; for example in the simulations done by Norrie *et al* [2–4] the cutoff used satisfied  $\Lambda a_s \approx 0.1$ .

Apart from the solitary case of hydrogen condensates, in all Bose–Einstein condensate experiments the scattering length  $a_s$  used to describe the interactions arises because of the existence of a weakly bound state of two atoms. The use of Feshbach resonances can give very large scattering lengths, consequently reducing the binding energy of this state to a very small value. This can introduce quite slow time scales, which makes it wise to investigate the possible influence of molecular dynamics on Bose–Einstein condensation phenomena.

The c-field method cannot be directly applied to any explicit description of the relevant molecular physics, since binding can only be described by an attractive potential, for which the Gross–Pitaevskii equation and similar c-field equations have no stable solutions, and certainly do not produce molecules. In this and subsequent papers, we want to combine the ideas of c-fields with those field theory methods which use an explicit “molecule field”, as originally introduced in [6, 7]. These kinds of models are purely phenomenological descriptions of the physics, whose parameters must be determined to reproduce the correct experimentally measurable quantities.

The two relevant parameters for the molecular field model are the *binding energy* of the weakly bound state, and the *s-wave scattering length*, which can be measured. We will therefore develop a method for relating them to the phenomenological parameters in our formalism. The effective range, we will argue, is not a useful parameter for characterizing the physics.

The formalism outlined in this paper is used in *Paper II* [8], where we implement the mean field theory in the Thomas-Fermi approximation, and the Bogoliubov theory for this model of a coupled atom-molecule system and use the latter to investigate the excitation spectrum for Bragg scattering from a uniform condensate. In *Paper III* [9] we implement this formalism numerically, performing full simulations of Bragg scattering from a trapped Bose-Einstein condensate, as in the recent experiment by [10]. The results from the Bogoliubov calculations and the full simulations both show that the measured effects on Bragg scattering as the scattering length increases are well described by our coupled atom-molecule formalism.

## 2 Effective Hamiltonian Method for Bose–Einstein Condensation

It is normal when describing Bose–Einstein condensation to use an approximate Hamiltonian for the system of ultra-cold atoms that gives a good description of only the long-wavelength behaviour of the system, which is all that is relevant for the observable physics. The relevant methods are called “pseudopotential methods” or “effective field theory methods”, and there is a long history associated with the various formulations of these methods [5, 11–13]. In all of these formulations, the underlying philosophy is to find an approximate description of the physics of very low energy particles. The definition of “low energy” in practice is that the scattering amplitude for such energies does not differ significantly from its value at zero energy.

It is best to formulate the concepts required precisely, and in a form adapted to the study of a trapped ultra-cold gas. In such a system all of the relevant physics involves particles with a finite small momentum—this means that we can restrict the description to particles with momentum less than a fixed cutoff value  $\hbar\Lambda$ . Consequently, the maximum *relative* momentum is  $2\hbar\Lambda$ , and for a given centre of mass momentum  $\mathbf{Q}$  of any pair of colliding particles the allowable values of relative momentum,  $\mathbf{p}$ , satisfy  $|\mathbf{p} + \frac{1}{2}\mathbf{Q}| \leq \Lambda$ . Thus the description of scattering of any pair of particles depends on their centre of mass momentum. If the possible values of  $\mathbf{Q}$  are themselves rather small in comparison with  $\hbar\Lambda$ , this dependence on the centre of mass momentum is not very important, and it is normally ignored.

The appropriate quantum field theory description in the case that the centre of mass dependence can be neglected is essentially that of Braaten and Nieto [5], and can be characterized as:

1. The system of atoms is described by a quantum field operator  $\hat{\psi}$ , defined on the low energy subspace specified by a momentum space cutoff  $\Lambda$

$$\hat{\psi}(\mathbf{x}) = \frac{1}{(2\pi)^{3/2}} \int_0^\Lambda d\mathbf{k} a_{\mathbf{k}} e^{i\mathbf{k}\cdot\mathbf{x}}. \quad (2)$$

2. The Hamiltonian for a trapped Bosonic gas of interacting particles is given by

$$H = \int d\mathbf{x} \left\{ \hat{\psi}^\dagger(\mathbf{x}) \left( -\frac{\hbar^2 \nabla^2}{2m} + V_a(\mathbf{x}) \right) \hat{\psi}(\mathbf{x}) + \frac{U}{2} \hat{\psi}^\dagger(\mathbf{x}) \hat{\psi}^\dagger(\mathbf{x}) \hat{\psi}(\mathbf{x}) \hat{\psi}(\mathbf{x}) \right\}, \quad (3)$$

where  $V_a$  is the trapping potential.

3. The quantity  $U$  is the inter-atomic scattering strength, and is related to the s-wave scattering length  $a_s$  by

$$U = \frac{4\pi\hbar^2 a_s}{m(1 - 2\Lambda a_s/\pi)}. \quad (4)$$

For the method to be useful it is necessary that  $2\Lambda a_s/\pi \ll 1$ , which will mean that the predictions of this Hamiltonian are independent of the cutoff, as long as this is not too large.<sup>1</sup> In this case, at sufficiently low temperatures, the condensate wavefunction  $\Psi(\mathbf{x}, t)$  is accurately described by the Gross–Pitaevskii equation

$$i\hbar \frac{\partial \Psi}{\partial t} = -\frac{\hbar^2 \nabla^2 \Psi}{2m} + V(\mathbf{x})\Psi + \frac{4\pi\hbar^2 a_s}{m} |\Psi|^2 \Psi. \quad (5)$$

<sup>1</sup>In fact, there is no reason to believe that the Hamiltonian (3) is valid unless this condition is satisfied.

Experimentally, this is a well-verified equation.

If  $2\Lambda a_s/\pi$  is not sufficiently small, the simple relationship between the Hamiltonian and the Gross–Pitaevskii equation disappears. The derivation of the Gross–Pitaevskii equation from the Hamiltonian involves higher order terms in perturbation theory, which the choice of a sufficiently small  $\Lambda$  implicitly sums.

It is important to emphasize that, although  $\Lambda$  is often called an “ultraviolet cutoff”, unlike such cutoffs in quantum electrodynamics, it has a finite value, and this value must be *small* for the pseudopotential Hamiltonian to be valid. Furthermore, in c-field methods, all states have at least half a quantum of occupation, so that all momenta up to  $\hbar\Lambda$  participate in calculations, and the corrections discussed in the appendix may be relevant.

### 3 An Effective Field Method for Molecules

Let us now introduce molecules into the c-field formalism. Since the Gross–Pitaevskii equation cannot produce bound states, it is clear that in some sense these molecules must be introduced “by hand”.

#### 3.1 The Molecular-Field Hamiltonian

A method used by several other groups [6, 7, 14–16], is to add an additional field  $\hat{\phi}$  corresponding to a molecule state, giving the Hamiltonian:

$$\hat{H} = \int d\mathbf{x} \left\{ \hat{\psi}^\dagger(\mathbf{x}) \left( -\frac{\hbar^2 \nabla^2}{2m} + V_a(\mathbf{x}) \right) \hat{\psi}(\mathbf{x}) + \hat{\phi}^\dagger(\mathbf{x}) \left( -\frac{\hbar^2 \nabla^2}{4m} + V_m(\mathbf{x}) + \varepsilon \right) \hat{\phi}(\mathbf{x}) + \frac{U_{aa}}{2} \hat{\psi}^\dagger(\mathbf{x}) \hat{\psi}^\dagger(\mathbf{x}) \hat{\psi}(\mathbf{x}) \hat{\psi}(\mathbf{x}) + U_{am} \hat{\psi}^\dagger(\mathbf{x}) \hat{\phi}^\dagger(\mathbf{x}) \hat{\phi}(\mathbf{x}) \hat{\psi}(\mathbf{x}) + \frac{U_{mm}}{2} \hat{\phi}^\dagger(\mathbf{x}) \hat{\phi}^\dagger(\mathbf{x}) \hat{\phi}(\mathbf{x}) \hat{\phi}(\mathbf{x}) + \frac{g}{2} \left( \hat{\phi}^\dagger(\mathbf{x}) \hat{\psi}(\mathbf{x}) \hat{\psi}(\mathbf{x}) + \hat{\psi}^\dagger(\mathbf{x}) \hat{\psi}^\dagger(\mathbf{x}) \hat{\phi}(\mathbf{x}) \right) \right\}. \quad (6)$$

Here the parameters have the interpretations

1.  $U_{aa}$  is the background atom interaction strength, leading to the concept of a background scattering length  $a_{bg} \equiv mU_{aa}/4\pi\hbar^2$ .
2.  $V_a$  and  $V_m$  are the external trapping potential for the atoms and the molecules respectively. If the magnetic moment of the weakly bound molecule is twice that of the atom, then  $V_m = 2V_a$ . However, this is not mandatory.
3.  $\varepsilon$  is an energy offset term, which allows for a finite binding energy of the molecule.
4. The coupling parameter  $g$  describes strength of coupling of the process by which a molecule is formed from two atoms.
5. The terms with factors  $U_{am}$  and  $U_{mm}$  correspond to atom-molecule and molecule-molecule scattering respectively. Since the atom field is usually much larger than the molecule field in the situations we shall consider, these terms are in most cases negligible.

##### 3.1.1 Phenomenology

The Hamiltonian (6), it must be emphasized, provides only a phenomenological description of the physics. In particular, the energy offset  $\varepsilon$  can be viewed as a representa-

tion of the effect of a Feshbach resonance, and is related to the binding energy of the molecule. However, the actual binding energy must be determined by solving the appropriate Schrödinger equation, and it will depend on the other parameters. Furthermore, for each value of  $\epsilon$ , the other parameters, and in particular  $g$ , may be different, and indeed, we will find that the values of  $g$  and  $\epsilon$  required to fit the measured scattering and binding properties are strongly interdependent. These dependencies in practice simply mean that when setting up a c-field simulation, one must choose the parameters appropriate to the experimental system under investigation.

In summary, the sole function of the Hamiltonian (6) is to provide a practical method of implementing c-field theory for molecules in a way that is consistent with measured properties of the atom-molecule system. The basic theory to which it is an approximation is a Hamiltonian involving only atoms interacting through an appropriate interatomic potential  $u(\mathbf{x} - \mathbf{x}')$ . The molecular field method is only necessary in this paper because the “exact” Hamiltonian cannot be represented inside a c-field theory.

### 3.1.2 Momentum Cutoffs

In this case of a coupled atom and molecule system there will be momentum cutoffs for both the molecular and the atomic fields, and these can be expressed in terms of projectors  $\mathcal{P}_a$  and  $\mathcal{P}_m$  that project the wavefunctions onto the low energy subspace below the cutoff. Because a molecule is formed from two atoms, the interactions will only make sense if the molecule cutoff is twice that of the atom. Thus, if the atom cutoff is  $\Lambda$ , the projectors can be defined as

$$\mathcal{P}_a(\mathbf{k}) = \Theta(\Lambda - |\mathbf{k}|), \quad (7)$$

$$\mathcal{P}_m(\mathbf{k}) = \Theta(2\Lambda - |\mathbf{k}|), \quad (8)$$

where  $\Theta$  is the Heaviside step function.

In (7,8) we have assumed isotropic cutoffs, but this is not necessarily the case for all systems. Indeed, as we shall see in *Paper III* in experimentally realistic systems the cutoff can be highly anisotropic. However, for the work in this paper, the exact properties of the cutoff are not relevant, and we therefore assume that it is isotropic.

## 4 Determination of Parameters

In order to determine the relationship between this formalism and reality, the parameters and the fields have to be related to physically observable quantities. To do this, we need to compute

1. The scattering amplitude,
2. The binding energy,
3. The bound state wavefunction.

### 4.1 Schrödinger Equation in the 2-Atom : 1-Molecule Sector

If  $|E\rangle$  is a state in 2-atom : 1-molecule sector, it has a two-component wavefunction, defined by the 2-atom amplitude

$$\psi(\mathbf{x}_1, \mathbf{x}_2) \equiv \langle 0 | \hat{\psi}(\mathbf{x}_1) \hat{\psi}(\mathbf{x}_2) | E \rangle, \quad (9)$$

and the 1-molecule amplitude

$$\phi(\mathbf{x}) \equiv \langle 0 | \hat{\phi}(\mathbf{x}) | E \rangle, \quad (10)$$

where  $|0\rangle$  is the vacuum state. The normalization of the wavefunctions is given by the condition

$$\int |\psi(\mathbf{x}_1, \mathbf{x}_2)|^2 d\mathbf{x}_1 d\mathbf{x}_2 + 2 \int |\phi(\mathbf{x})|^2 d\mathbf{x} = 1. \quad (11)$$

We write the Schrödinger equation for the atom and molecule wavefunctions corresponding to the Hamiltonian (6) as

$$E\psi(\mathbf{x}_1, \mathbf{x}_2) = -\frac{\hbar^2 (\nabla_1^2 + \nabla_2^2)}{2m} \psi(\mathbf{x}_1, \mathbf{x}_2) + \delta(\mathbf{x}_1 - \mathbf{x}_2) (U_{aa}\psi(\mathbf{x}_1, \mathbf{x}_2) + g\phi(\mathbf{x}_1)), \quad (12)$$

$$E\phi(\mathbf{x}) = -\frac{\hbar^2 \nabla^2}{4m} \phi(\mathbf{x}) + \varepsilon\phi(\mathbf{x}) + \frac{g}{2} \psi(\mathbf{x}, \mathbf{x}). \quad (13)$$

The equivalent Schrödinger equations for the momentum space wavefunctions  $\tilde{\psi}$  and  $\tilde{\phi}$  take the form

$$\left( E - \frac{\hbar^2}{2m} (p_1^2 + p_2^2) \right) \tilde{\psi}(\mathbf{p}_1, \mathbf{p}_2) = \frac{U_{aa}}{(2\pi)^3} \int_0^\Lambda d\mathbf{q}_1 \int_0^\Lambda d\mathbf{q}_2 \delta(\mathbf{q}_1 + \mathbf{q}_2 - \mathbf{p}_1 - \mathbf{p}_2) \tilde{\psi}(\mathbf{q}_1, \mathbf{q}_2) + g\tilde{\phi}(\mathbf{p}_1 + \mathbf{p}_2), \quad (14)$$

$$\left( E - \varepsilon - \frac{\hbar^2 p^2}{4m} \right) \tilde{\phi}(\mathbf{p}) = \frac{g}{2(2\pi)^3} \int_0^\Lambda d\mathbf{q}_1 \int_0^\Lambda d\mathbf{q}_2 \delta(\mathbf{q}_1 + \mathbf{q}_2 - \mathbf{p}) \tilde{\psi}(\mathbf{q}_1, \mathbf{q}_2). \quad (15)$$

We transform the coordinate system to one of center-of-mass and relative momenta by the substitutions  $\mathbf{P} = \mathbf{p}_1 + \mathbf{p}_2$ ,  $\mathbf{P}' = \mathbf{q}_1 + \mathbf{q}_2$ ,  $\mathbf{k} = (\mathbf{p}_1 - \mathbf{p}_2)/2$  and  $\mathbf{k}' = (\mathbf{q}_1 - \mathbf{q}_2)/2$ . In the centre of mass frame where  $\mathbf{P} = 0$  the equations take the form

$$\left( E - \frac{\hbar^2 k^2}{m} \right) \tilde{\psi}(\mathbf{k}) = \frac{U_{aa}}{(2\pi)^3} \int_0^\Lambda d\mathbf{k}' \tilde{\psi}(\mathbf{k}') + g\tilde{\phi}(0), \quad (16)$$

$$(E - \varepsilon) \tilde{\phi}(0) = \frac{g}{2(2\pi)^3} \int_0^\Lambda d\mathbf{k}' \tilde{\psi}(\mathbf{k}'), \quad (17)$$

where we have redefined  $\tilde{\psi}$  as the one component momentum space wavefunction for the atomic field.

The projectors (7,8) define a preferred frame; in a frame in which  $\mathbf{P} \neq 0$ , the range of the momentum integrals becomes  $|\mathbf{k} + \frac{1}{2}\mathbf{P}| \leq \Lambda$ . Since the most important interactions in a Bose–Einstein condensate do correspond to very small centre of mass momentum (see appendix), this is not a great problem.

#### 4.1.1 The Yamaguchi Equation

Substituting the molecule function (17) into the atom equation (16), we obtain

$$\left( \frac{Em}{\hbar^2} - k^2 \right) \tilde{\psi}(\mathbf{k}) = \lambda(E) \int_0^\Lambda d\mathbf{k}' \tilde{\psi}(\mathbf{k}'), \quad (18)$$

where

$$\lambda(E) = \frac{m}{(2\pi)^3 \hbar^2} \left( U_{aa} + \frac{g^2/2}{E - \varepsilon} \right). \quad (19)$$

Equation (18) is similar in form to Yamaguchi's separable potential equation [17], with the important difference that our expression has an explicit dependence on the energy eigenvalue  $E$  in the  $\lambda$  factor. However, the method of solution is essentially unaltered.

#### 4.1.2 Scattering state solution

A scattering state will be characterized by a positive energy eigenvalue, so we make the substitution  $E \rightarrow \hbar^2 K^2/m$  in (18), which can now be written as

$$\tilde{\psi}(\mathbf{k}) = \delta(\mathbf{K} - \mathbf{k}) + \frac{\lambda_K}{K^2 - k^2 + i\eta} \int_0^\Lambda d\mathbf{k}' \tilde{\psi}(\mathbf{k}'), \quad (20)$$

where we have defined  $\lambda_K \equiv \lambda(\hbar^2 K^2/m)$ . Integrating over  $\mathbf{k}$  on both sides gives the result

$$\int_0^\Lambda d\mathbf{k} \tilde{\psi}(\mathbf{k}) = \left( 1 - \lambda_K \int_0^\Lambda d\mathbf{k} \frac{1}{K^2 - k^2 + i\eta} \right)^{-1}. \quad (21)$$

**Small  $K$  Approximation** The integral on the right hand side can be evaluated exactly, and for  $K \ll \Lambda$  approximated thus:

$$\int_0^\Lambda d\mathbf{k} \frac{1}{K^2 - k^2 + i\eta} = -4\pi\Lambda - 2i\pi^2 K + 2\pi K \ln\left(\frac{\Lambda + K}{\Lambda - K}\right) \approx -4\pi\Lambda - 2i\pi^2 K + 4\pi \frac{K^2}{\Lambda}. \quad (22)$$

The atom wavefunction for the scattering state can therefore be written as

$$\tilde{\psi}(\mathbf{k}) = \delta(\mathbf{K} - \mathbf{k}) - \frac{1}{(-1/\lambda_K - 4\pi\Lambda - 2i\pi^2 K + 4\pi K^2/\Lambda)} \frac{1}{(K^2 - k^2 + i\eta)}. \quad (23)$$

Similarly, the solution for the molecular wavefunction is given by

$$\begin{aligned} \tilde{\phi}(0) &= \frac{g/2}{\hbar^2 K^2/m - \varepsilon} \int_0^\Lambda d\mathbf{k}' \tilde{\psi}(\mathbf{k}') = \\ &= \frac{g/2}{(\hbar^2 K^2/m - \varepsilon)} \frac{1}{(-1 + \lambda_K(4\pi\Lambda + 2i\pi^2 K - 4\pi K^2/\Lambda))}. \end{aligned} \quad (24)$$

**Effective Range and Scattering Length** The scattering wavefunction for incident momentum  $\mathbf{K}$  and final momentum  $\mathbf{k}$  is

$$\tilde{a}_K(\mathbf{k}) \equiv \delta(\mathbf{K} - \mathbf{k}) - \frac{f(\mathbf{k}, \mathbf{K})}{2\pi^2(K^2 - k^2 + i\eta)}, \quad (25)$$

where  $f(\mathbf{k}, \mathbf{K})$  is the scattering amplitude and is thus given by

$$f(\mathbf{k}, \mathbf{K}) = \frac{-2\pi^2 \lambda_K}{1 - \lambda_K \int_0^\Lambda d\mathbf{k} \frac{1}{K^2 - k^2 + i\eta}} = \left( -\frac{1}{2\pi^2 \lambda_K} - \frac{2}{\pi} \Lambda - iK + \frac{1}{\pi} K \ln\left(\frac{\Lambda + K}{\Lambda - K}\right) \right)^{-1}. \quad (26)$$

The scattering amplitude for small incident momenta can be approximated by the effective range expansion,

$$f(K) = \frac{1}{K \cot \delta - iK} \approx \frac{1}{-1/a_s - iK + r_0 K^2/2}, \quad (27)$$

where  $\delta$  is the phase shift,  $a_s$  is the s-wave scattering length and  $r_0$  is the effective range of the potential. We expand (26) for small  $K$  using the expansions

$$\frac{1}{\lambda_K} \approx \frac{(2\pi)^3 \hbar^2}{m} \left( U_{aa} - \frac{g^2}{2\varepsilon} \right)^{-1} + \pi K^2 \left( \frac{4\pi \hbar^2}{m} \frac{g^2/2\varepsilon}{g(U_{aa} - g^2/2\varepsilon)} \right)^2, \quad (28)$$

$$\ln \left( \frac{\Lambda + K}{\Lambda - K} \right) \approx \frac{2K}{\Lambda}, \quad (29)$$

where (29) is valid as long as

$$K \ll \Lambda, \quad (30)$$

and (28) is valid as long as

$$\frac{\hbar^2 K^2}{m} \ll \frac{g^2}{2U_{aa}} - \varepsilon. \quad (31)$$

We can thus use equations (26) and (27) to identify

$$a_s = \left[ \frac{4\pi \hbar^2}{m} \left( U_{aa} - \frac{g^2}{2\varepsilon} \right)^{-1} + \frac{2}{\pi} \Lambda \right]^{-1}, \quad (32)$$

$$r_0 = \frac{4}{\pi \Lambda} - \frac{1}{\pi} \left( \frac{4\pi \hbar^2}{m} \frac{g/2\varepsilon}{(U_{aa} - g^2/2\varepsilon)} \right)^2. \quad (33)$$

**Background Scattering Length** Setting  $g^2/\varepsilon \rightarrow 0$  in (32) corresponds to the case when the effect of the Feshbach resonance is negligible; ie, only the background scattering term is nonzero. This means that the background scattering length is

$$a_{bg} = \left[ \frac{4\pi \hbar^2}{m U_{aa}} + \frac{2}{\pi} \Lambda \right]. \quad (34)$$

### 4.1.3 Nature of Effective Range Expansion

The effective range expansion of the scattering amplitude has the rather limited range of validity—the two conditions (30, 31) set an upper bound for  $K$ , and for the expansion to be quantitatively valid,  $K$  must lie well inside the region defined by the intersection of the spaces determined by these bounds. The situation is illustrated in Fig. 1 for parameters appropriate to the problems we wish to study, for which available  $K$ -space is limited by the bound determined by  $\Lambda$ , that is, by the dashed circle.

However, the exact solution (26) for the scattering amplitude possesses singularities at  $K = \pm\Lambda$ , but is analytic for imaginary values of  $K$  with modulus very much greater than  $\Lambda$ . In fact, the bound state solution to the scattering problem is given by the pole of (26) on the negative imaginary axis and, in cases we consider, is well outside the region bounded by the dashed line. This pole cannot be obtained by making the effective range expansion (27) for the scattering amplitude. (In fact in Section 4.2 we will find it more convenient to determine the bound state properties by direct solution of the scattering equation, rather than by direct evaluation of the position and residue of the pole, which is fully equivalent to determining the pole and its residue). We will therefore interpret the available  $K$ -space region as the asymmetric region bound by the cutoff  $\Lambda$  on the real axis, but including the bound state on the imaginary axis, indicated by the shaded area in Fig. 1.



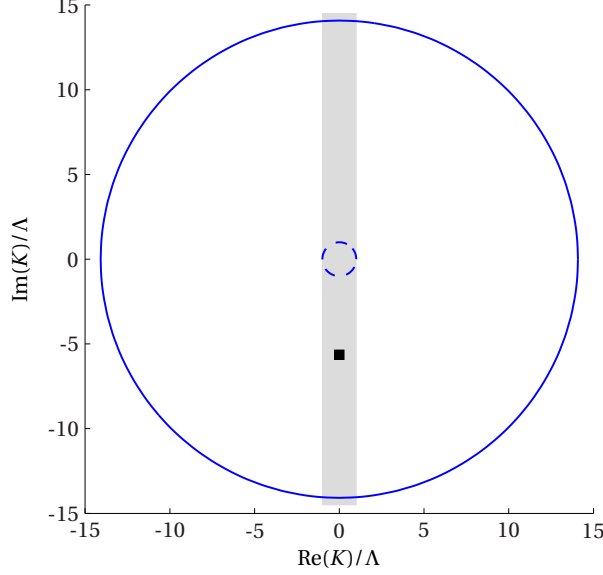


Figure 1: The grey region shows the region of validity for the scattering amplitude (26) in the complex plane. The upper bounds (30, 31) for the individual expansions (28, 29) are given as the dashed and solid circles respectively. The region of validity for the effective range expansion is obviously situated within the smaller of these, while the bound state solution (black square) can be found far outside this area. The plot here is for a cutoff value of  $\Lambda = 2.2 \times 10^6$  and a scattering length of  $a = 900a_0$ , but we get qualitatively similar results for the whole parameter range used in this paper.

With the model we have chosen, it is not possible to simultaneously fit the binding energy, the scattering length and the effective range, since there are only two fitting parameters,  $g$  and  $\varepsilon$ . The scattering length and binding energy are the relevant measurable parameters for the kind of problem we wish to study, whereas the effective range does not play any direct role, and therefore we will determine  $g$  and  $\varepsilon$  by fitting the measured values of scattering length and binding energy. In this paper, we will not concern ourselves any further with the effective range.

## 4.2 Bound state solution

In this atom-molecule model, a physical bound state will be a superposition of a state of two  $\psi$ -field “atoms”, and a state of one  $\phi$ -field “molecule”. A bound state solution is characterized by a negative energy eigenvalue,  $E \rightarrow -\hbar^2 \alpha^2 / m$  in (18), where  $\alpha^2 > 0$ , so that  $K \rightarrow (0, i\alpha)$ . Equation (18) can now be written as

$$\tilde{\psi}(\mathbf{k}) = -\frac{\lambda_\alpha}{\alpha^2 + k^2} \int_0^\Lambda d\mathbf{k}' \tilde{\psi}(\mathbf{k}'), \quad (35)$$

where we have defined  $\lambda_\alpha$  by setting  $E \rightarrow -\hbar^2 \alpha^2 / m$  in (19). By taking the integral over  $\mathbf{k}$  on both sides, we can remove the dependence on the wavefunction, to get

$$1 = -4\pi \int_0^\Lambda \frac{\lambda_\alpha k^2}{\alpha^2 + k^2} dk = -4\pi \lambda_\alpha \left[ \Lambda - \alpha \arctan\left(\frac{\Lambda}{\alpha}\right) \right], \quad (36)$$

so that  $\alpha$ , and hence the binding energy, are determined by the solution of the equation

$$\alpha \arctan\left(\frac{\Lambda}{\alpha}\right) = \left[ \frac{m}{2\pi^2 \hbar^2} \left( U_{aa} + \frac{g^2/2}{-\hbar^2 \alpha^2 / m - \varepsilon} \right) \right]^{-1} + \Lambda. \quad (37)$$

**Threshold of binding** At the bound state threshold, where  $\alpha \rightarrow 0$ , we can solve (37) exactly in terms of  $\varepsilon$  to give

$$\varepsilon_{\text{threshold}} = \frac{g^2}{2} \left[ U_{aa} + \frac{2\pi^2 \hbar^2}{m\Lambda} \right]^{-1}, \quad (38)$$

which is of course identical to the solution of the scattering length equation (32) when  $a_s = 0$ . Substituting from (34), this takes the form

$$\varepsilon_{\text{threshold}} = \left( \frac{g^2}{2} \right) \left( \frac{m}{4\pi\hbar^2} \right) \frac{\pi/2\Lambda}{1 - 2\Lambda a_{bg}/\pi}. \quad (39)$$

This is nonzero unless  $g^2 \rightarrow 0$  at threshold.

**Weakly bound molecules** For small values of  $\alpha$  we can expand the left hand side of (37) to give

$$\alpha \left( \frac{\pi}{2} - \frac{\alpha}{\Lambda} \right) = \left[ \frac{m}{2\pi^2 \hbar^2} \left( U_{aa} + \frac{g^2/2}{-\hbar^2 \alpha^2/m - \varepsilon} \right) \right]^{-1} + \Lambda, \quad (40)$$

so that we get for weakly bound molecules

$$\alpha \approx \left[ \frac{m}{4\pi\hbar^2} \left( U_{aa} + \frac{g^2/2}{-\varepsilon} \right) \right]^{-1} + \frac{2}{\pi} \Lambda. \quad (41)$$

It is clear that in the case of weakly bound molecules  $\alpha \approx 1/a_s$ , as expected from the relationship between the binding energy and the scattering length for sufficiently small binding energies.

**Tightly bound molecules** For large values of  $\alpha$ , expanding  $\arctan(\Lambda/\alpha)$  in (37) yields

$$\alpha \left( \frac{\Lambda}{\alpha} - \frac{\Lambda^3}{3\alpha^3} \right) \approx \left[ \frac{m}{2\pi^2 \hbar^2} \left( U_{aa} - \frac{g^2/2}{\hbar^2 \alpha^2/m + \varepsilon} \right) \right]^{-1} + \Lambda, \quad (42)$$

so that we instead get

$$\alpha^2 \approx -\frac{m\varepsilon}{\hbar^2} + \frac{\pi^2 \hbar^2 \Lambda^3 g^2}{3m} \left( \frac{2\pi^2 \Lambda^3 U_{aa}}{3} + \varepsilon \right)^{-1}. \quad (43)$$

For sufficiently large values of  $\varepsilon$  we have that  $\alpha^2 \approx -m\varepsilon/\hbar^2$ , which means that the detuning  $\varepsilon$  is approximately equal to the binding energy  $E_b = \hbar^2 \alpha^2/m$  for large values of the detuning, as would be expected.

#### 4.2.1 Atomic Fraction of the Bound State

The bound state solution for the atom wavefunction is

$$\tilde{\psi}(\mathbf{k}) = \frac{N}{\alpha^2 + k^2}, \quad (44)$$

where, if the normalization is chosen to be  $\int d^3 \mathbf{k} |\tilde{\psi}(\mathbf{k})|^2 = M$ , the factor  $N$  will be given by

$$\frac{M}{N^2} = \int_0^\Lambda d\mathbf{k} \frac{1}{(\alpha^2 + k^2)^2} = 4\pi \int_0^\Lambda \frac{k^2}{(\alpha^2 + k^2)^2} dk = 2\pi \left[ \frac{1}{\alpha} \arctan\left(\frac{\Lambda}{\alpha}\right) - \frac{\Lambda}{\Lambda^2 + \alpha^2} \right]. \quad (45)$$

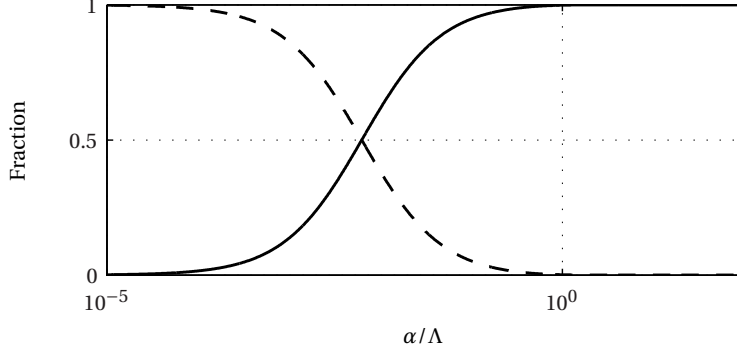


Figure 2: The fractions of the atom pairs (dashed line) and elementary molecules (solid line). The values of the length parameters are in this case those for  $^{85}\text{Rb}$ ; namely  $l_{ug} \approx 10^{-7}$ ,  $a_{bg} = -2.32 \times 10^{-8}$ , and we have chosen  $\Lambda = 2 \times 10^6$ .

Similarly the solution for the molecular state can be obtained by substituting (44) into (17), giving

$$\tilde{\phi}(0) = -\frac{g}{2(\hbar^2\alpha^2/m + \varepsilon)} \int_0^\Lambda d\mathbf{k}' \tilde{\psi}(\mathbf{k}'), \quad (46)$$

$$= -\frac{2\pi g N}{\hbar^2\alpha^2/m + \varepsilon} \left[ \Lambda - \alpha \arctan\left(\frac{\Lambda}{\alpha}\right) \right], \quad (47)$$

$$= \frac{4\pi N}{g} \left( U_{aa} \left( \alpha \arctan\left(\frac{\Lambda}{\alpha}\right) - \Lambda \right) - \frac{2\pi^2 \hbar^2}{m} \right), \quad (48)$$

where we have used (37) to get to the last line.

The ratio of the probabilities for the atom and the molecule states can then be written

$$\frac{P_{\text{mol}}}{P_{\text{atm}}} = \frac{|\phi(0)|^2}{\int d\mathbf{k} |\tilde{\psi}(\mathbf{k})|^2} = 8\pi \left(\frac{\alpha}{\Lambda}\right)^2 (l_{ug}\Lambda)^3 \left( \frac{(t(\alpha/\Lambda) - \pi/2\Lambda a_{bg})^2}{t(\alpha/\Lambda) + \Lambda^2/(\Lambda^2 + \alpha^2)} \right), \quad (49)$$

where

$$t(z) \equiv z \arctan(1/z) - 1, \quad (50)$$

$$l_{ug} \equiv \left( \frac{U_{aa}}{g} \right)^{2/3}. \quad (51)$$

The result depends on the four parameters which are all lengths, namely  $l_{ug}$ ,  $a_{bg}$ ,  $\Lambda^{-1}$  and  $\alpha^{-1}$ . It is worth noting that while it is mandatory that  $|K|/\Lambda$  be less than 1, the same is not true for  $|\alpha|/\Lambda$ , which does not necessarily have to be less than 1. On the contrary, in most experiments the binding energy is usually such that  $|\alpha| \gg \Lambda$ , for realistic values of the cutoff (cf. Section 4.1.3).

The parameter  $\alpha^{-1}$  determines the spatial extent of the atom-pair part of the wavefunction of the bound state, and this can only be represented on the spatial grid corresponding to the cutoff  $\Lambda$  if  $\alpha/\Lambda \ll 1$ . The crossover from the predominantly atom-pair wavefunction to the elementary molecule wavefunction corresponds to the molecular size becoming smaller than the size of the spatial grid. However, (49) shows that, as well as  $\Lambda^{-1}$ , there are the other lengths  $a_{bg}$  and  $l_{ug}$  which also come into play. This means that the intuitive idea that the crossover happens at  $\alpha/\Lambda \approx 1$  is significantly modified,

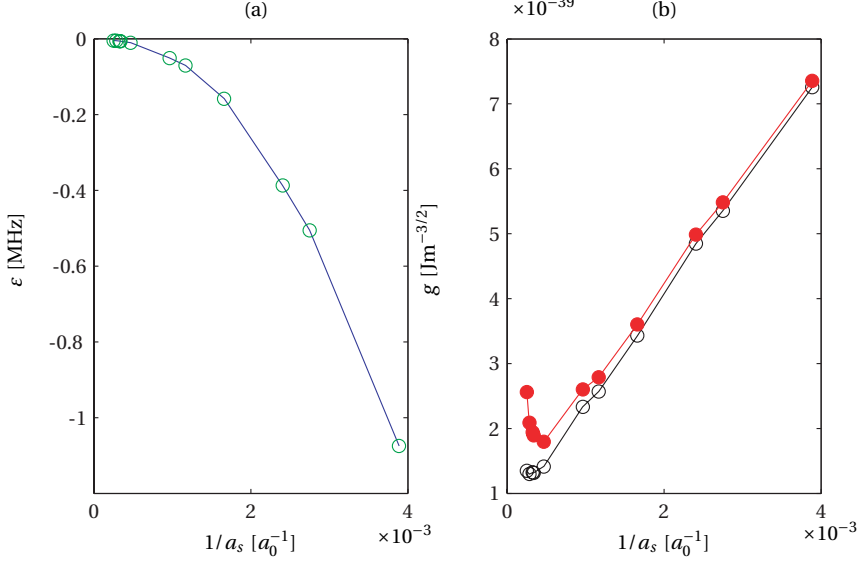


Figure 3: Values in SI units of the parameters a)  $g$ , and b)  $\epsilon$  in the Hamiltonian (6), as calculated from (32) and (37) for cutoff values  $\Lambda = 2.2 \times 10^6 \text{m}^{-1}$  (hollow black circles) and  $\Lambda = 1 \times 10^7 \text{m}^{-1}$  (solid red circles). For (a) only values of  $\epsilon$  corresponding to  $\Lambda = 2.2 \times 10^6$  are plotted, since the values of  $\epsilon$  for the two different values  $\Lambda$  are almost indistinguishable from each other. In both plots the parameters are calculated using data of the binding energy and scattering length taken from [18]. Solid lines are to guide the eye.

and in Fig. 2, which shows the fractions of the atom and the molecule states as functions of  $\alpha/\Lambda$ , it can be seen that the crossover is closer to  $\alpha/\Lambda \approx 0.01$ .

The crossover is thus explicitly cutoff dependent, but this is purely a technical issue. There is no fundamental physics in this crossover; it is determined simply by the technical need to have a cutoff. This has to be sufficiently large to represent the spatial features under investigation, and also has an upper bound determined by the requirement that  $\Lambda a_s$  be much less than one. However, within this range it is arbitrary.

### 4.3 Determination of Parameters

Of the parameters in the Hamiltonian (6) necessary for our modelling,  $g$ ,  $\epsilon$  and  $U_{aa}$ , it is only the last that can be directly determined experimentally, since the background scattering length  $a_{bg}$  is given by (34). The coupling  $g$  and the energy detuning  $\epsilon$ , however, need to be derived from other physically measurable quantities.

The s-wave scattering length  $a_s$  is well known for most condensate systems, and for  $^{85}\text{Rb}$  the molecular binding energy  $E_b \equiv \hbar^2 \alpha^2 / m$  has been measured for a range of magnetic fields which covers that used to vary the scattering length by means of a Feshbach resonance. Thus, a range of corresponding experimental values of  $a_s, \alpha$  exists, and matching these to the expressions (32) and (37), it is possible to determine the necessary sets of values of  $g$  and  $\epsilon$  for a chosen value of the cutoff  $\Lambda$  in the form

$$\epsilon = \left( \frac{\hbar^2 \alpha^2}{2m} \right) \frac{(\pi - 2\Lambda a_s)(1 - 2\Lambda t(\alpha/\Lambda) a_{bg}/\pi)}{\Lambda a_s(1 + t(\alpha/\Lambda)) - \pi}, \quad (52)$$

$$g^2 = \left( \frac{8\pi \hbar^4 \alpha^2}{m^2} \right) \frac{(a_{bg}(\pi - 2\Lambda a_s) - \pi a_s)(1 - 2\Lambda t(\alpha/\Lambda) a_{bg}/\pi)}{2\Lambda a_s(1 + t(\alpha/\Lambda)) - \pi}. \quad (53)$$

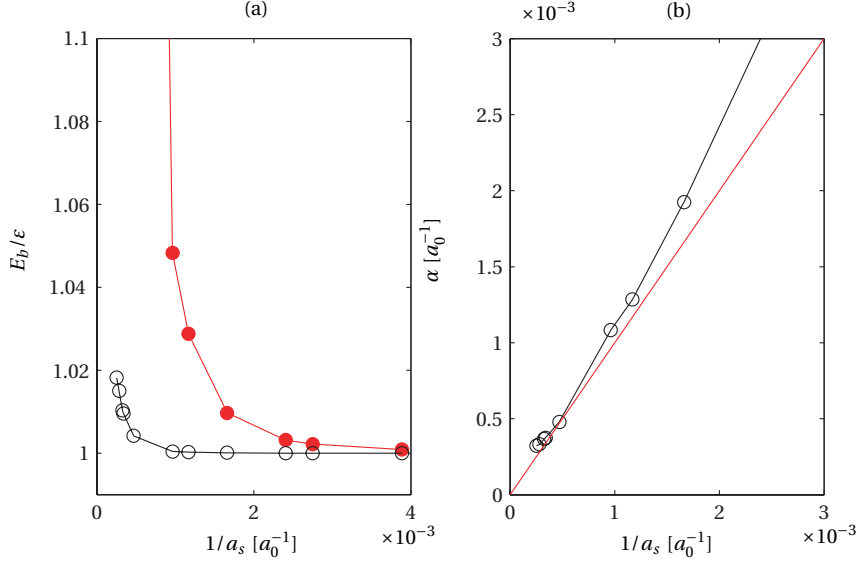


Figure 4: a) The ratio  $E_b/\varepsilon$  plotted for cutoff values  $\Lambda = 2.2 \times 10^6 \text{m}^{-1}$  (hollow black circles) and  $\Lambda = 1 \times 10^7 \text{m}^{-1}$  (solid red circles). This ratio is seen to be very close to 1, deviating only at scattering lengths more than of about  $5 \times 10^{-8} \text{m} \approx 1000 a_{\text{Bohr}}$ . The deviation at larger scattering lengths depends strongly on the choice of cutoff  $\Lambda$ , and is also affected by mean field effects; b) Plot of  $\alpha$  vs.  $a_s^{-1}$ ; the value of  $\alpha$  must approach  $a_s^{-1}$  for sufficiently small  $\alpha$ . However, the data used for these plots is measured in a Bose–Einstein condensate, and the four points corresponding to  $a_s^{-1} < 1 \times 10^7 \text{m}^{-1}$  deviate from this law because of mean field effects specific to that situation. In both plots the parameters are calculated using data of the binding energy and scattering length taken from [18].

In Fig. 3 we show the Hamiltonian parameters as functions of the s-wave scattering length calculated in this way for two different values of the cutoff  $\Lambda$ , using data of the binding energy and scattering length taken from [18]. The dependence on  $\Lambda$  is seen to be quite weak. (In applications to c-field calculations, the cutoff is related to the size of the simulation grid and it is important to choose the grid such that  $a_s$  and  $E_b$  depend only weakly on the value of  $\Lambda$ .)

Figs. 3 and 4 also show that the parameter  $g$  is essentially a linear function of  $a_s^{-1}$ , while energy offset  $\varepsilon$  is almost proportional to the binding energy  $E_b$ . Looking at Fig. 4, it can be seen that  $E_b$  and  $\varepsilon$  are essentially equal except for the very small binding energies which occur at large  $a_s$ . In fact, since the data show that  $g$  is unlikely to be zero at the threshold of binding, where  $a_s^{-1} \rightarrow 0$ , it can be seen from (38) that  $\varepsilon_{\text{threshold}} \neq 0$ , and given that for  $^{85}\text{Rb}$  the background scattering length is negative, the threshold value of  $\varepsilon$  is in fact positive.

In panel b) of Fig. 4, it can also be seen that  $a_s^{-1}$  and  $\alpha$  become very close, but when equality approaches at weak binding, the mean field effect of the Bose–Einstein condensate used in the experimental measurement obscures the equality, which was also noted in [18].

#### 4.4 Validity of the Effective range Expansion

Using (52) and (53) we can now estimate the validity of the effective range expansion in section 4.1.2. In Fig. 5 we plot the ratio of the effective range expansion  $K \cot \delta \approx 1/a_s + r_0 K^2/2$  and the exact expression for  $K \cot \delta$ , given by the inverse of the real part of the

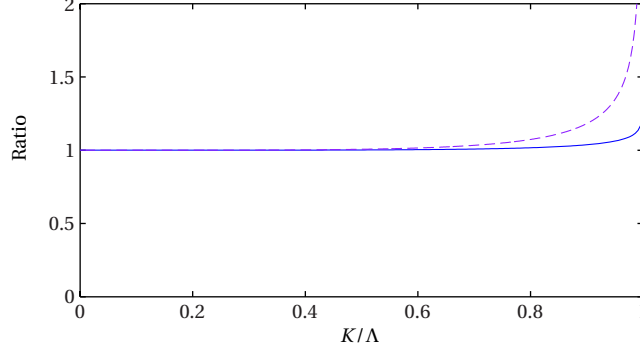


Figure 5: Ratio of the effective range expansion and the exact expression for  $K \cot \delta$ . The dash-dotted purple line corresponds to  $\Lambda = 10^7$  and the blue solid line corresponds to  $\Lambda = 2.2 \times 10^6$ . The scattering length is set to  $a_s = 900a_0$  and the effective range is given by equation (33).

right hand side of (26). We can easily see that the effective range expansion is only valid up to  $K \approx 0.6\Lambda$ .

## 5 Conclusion

The Hamiltonian (6) can thus be used to simulate realistic atom-molecule systems, as long as the *binding energy and s-wave scattering length are known. It is not important to match the value of the effective range, which in this kind of model is determined by the value of the cutoff, and has little physical significance.* The mapping of these physically observable parameters to the phenomenological parameters in the Hamiltonian will be dependent on the choice of the cutoff, but the results obtained in simulations should be essentially independent of the choice of  $\Lambda$ .

In *Paper II* and *Paper III*, we will apply the model Hamiltonian we have formulated here to the application of c-field methods to:

1. The formulation (for this model) of the simplest mean-field theory, and in particular the Thomas-Fermi approximation to the profile of a trapped condensate.
2. The study of the excitation spectrum of Bose–Einstein condensates and application to Bragg scattering of a homogeneous system;
3. The modelling of Feshbach-resonance-enhanced Bragg scattering from a trapped inhomogeneous Bose–Einstein condensate.

We will demonstrate that the experimental data from [10] can be reproduced accurately.

## Acknowledgments

The research in this paper was supported by the New Zealand Foundation for Research, Science and Technology under Contract No. NERF-UOOX0703, “Quantum Technologies”, Marsden Contract No. UOO509.

## A Corrections to the Scattering Length and Binding Energy for Non-Zero Centre of Mass Momentum

In Section 4.1 we assume that the centre of mass momentum of the system is zero, and thus we solve the integral in (18) on the range  $[0, \Lambda]$ . In this appendix we are investigating the corrections that occur when the centre of mass momentum is non-zero.

### A.1 Scattering length

To find the corrections to the scattering length, we wish to evaluate the integral in (21)

$$\mathcal{J}_s = \int_{\mathcal{R}_Q} d\mathbf{q} \frac{1}{K^2 - q^2 + i\eta} \quad (54)$$

where the range  $\mathcal{R}_Q$  is now defined by

$$|\mathbf{Q} \pm 2\mathbf{q}| \leq 2\Lambda, \quad (55)$$

for the centre of mass momentum  $\hbar\mathbf{Q} \equiv \mathbf{p}_1 + \mathbf{p}_2 = \mathbf{p}_3 + \mathbf{p}_4$ .

We change the integral to polar coordinates, so that the range  $\mathcal{R}_Q$  is equivalent to

$$Q^2 + 4q^2 \pm 4qQ \cos\theta \leq 4\Lambda^2 \quad (56)$$

$$\Rightarrow |\cos\theta| \leq X \equiv \min\left(1, \frac{4\Lambda^2 - Q^2 - 4q^2}{4qQ}\right). \quad (57)$$

Thus, we can write

$$\mathcal{J}_s = 2\pi \int_0^{\sqrt{\Lambda^2 - Q^2/4}} \frac{q^2}{K^2 - q^2 + i\eta} dq \int_0^X 2d\cos\theta \quad (58)$$

$$= 4\pi \int_0^{\sqrt{\Lambda^2 - Q^2/4}} \frac{q^2}{K^2 - q^2 + i\eta} dq \min\left(1, \frac{4\Lambda^2 - Q^2 - 4q^2}{4qQ}\right). \quad (59)$$

Noting that the point at which  $(4\Lambda^2 - Q^2 - 4q^2)/4mqQ = 1$  is when  $q = 2\Lambda - Q$ , we can write

$$\begin{aligned} \mathcal{J}_s &= 4\pi \int_{\Lambda - Q/2}^{\sqrt{\Lambda^2 - Q^2/4}} \frac{q^2}{K^2 - q^2 + i\eta} \frac{4\Lambda^2 - Q^2 - 4q^2}{4qQ} dq \\ &\quad + 4\pi \int_0^{\Lambda - Q/2} \frac{q^2}{K^2 - q^2 + i\eta} dq, \end{aligned} \quad (60)$$

$$\begin{aligned} &= 4\pi \left( \frac{\Lambda}{2} - \frac{Q}{4} + \frac{\Lambda^2 - Q^2/4 - K^2/2}{2Q} \ln \left| \frac{K^2 - (\Lambda - Q/2)^2}{K^2 - \Lambda^2 + Q^2/4} \right| \right) \\ &\quad + 4\pi \left( -\Lambda + \frac{Q}{2} - \frac{i\pi}{2}K + \frac{K}{2} \ln \left| \frac{K + \Lambda - Q/2}{K - \Lambda + Q/2} \right| \right) \end{aligned} \quad (61)$$

$$\begin{aligned} &= -2\pi\Lambda + \pi Q - 2i\pi^2 K + 2\pi \frac{\Lambda^2 - Q^2/4 - K^2/2}{Q} \ln \left| \frac{K^2 - (\Lambda - Q/2)^2}{K^2 - \Lambda^2 + Q^2/4} \right| \\ &\quad + 2\pi K \ln \left| \frac{K + \Lambda - Q/2}{K - \Lambda + Q/2} \right|. \end{aligned} \quad (62)$$

In the case when  $K \ll \Lambda$ , we can set  $K \rightarrow 0$  in (62) and the expression for the scattering amplitude becomes

$$f = \frac{-2\pi^2 \lambda_K}{1 - \lambda_K \mathcal{J}_s} = \left( -\frac{1}{2\pi^2 \lambda_K} - \frac{\Lambda}{\pi} + \frac{Q}{2\pi} + \frac{1}{\pi} \frac{\Lambda^2 - Q^2/4}{Q} \ln \left| \frac{\Lambda - Q/2}{\Lambda + Q/2} \right| \right)^{-1}, \quad (63)$$

giving us the following expression for the scattering length,

$$a_s = \left[ \frac{4\pi \hbar^2}{m} \left( U_{aa} - \frac{g^2}{2\varepsilon} \right)^{-1} + \frac{\Lambda}{\pi} - \frac{Q}{2\pi} - \frac{1}{\pi} \frac{\Lambda^2 - Q^2/4}{Q} \ln \left| \frac{\Lambda - Q/2}{\Lambda + Q/2} \right| \right]^{-1}. \quad (64)$$

For  $Q \ll 2\Lambda$ , this can be approximated by

$$a_s \approx \left[ \frac{4\pi \hbar^2}{m} \left( U_{aa} - \frac{g^2}{2\varepsilon} \right)^{-1} + \frac{2}{\pi} \Lambda - \frac{Q}{2\pi} - \frac{Q^2}{6\pi\Lambda} \right]^{-1}. \quad (65)$$

Thus, the consequence of a non-zero  $Q$  is a reduction in the effective value of  $\Lambda$ . However, this reduction will have very little impact on the value of the scattering length, since in practice  $\Lambda$  must be chosen to reduce any such effects.

## A.2 Binding Energy

To find the correction to the binding energy, we wish to solve the integral in (36)

$$\mathcal{J}_b = \int_{\mathcal{R}_Q} d\mathbf{q} \frac{1}{\alpha^2 + q^2}, \quad (66)$$

where the range  $\mathcal{R}_Q$  is now defined by

$$|\mathbf{Q} \pm 2\mathbf{q}| \leq 2\Lambda, \quad (67)$$

for the centre of mass momentum  $\hbar\mathbf{Q} \equiv \mathbf{p}_1 + \mathbf{p}_2 = \mathbf{p}_3 + \mathbf{p}_4$ .

Following the same method as above, we can write the integral as

$$\mathcal{J}_b = 4\pi \int_{\Lambda-Q/2}^{\sqrt{\Lambda^2 - Q^2/4}} \frac{q^2}{\alpha^2 + q^2} \frac{4\Lambda^2 - Q^2 - 4q^2}{4qQ} dq + 4\pi \int_0^{\Lambda-Q/2} \frac{q^2}{\alpha^2 + q^2} dq, \quad (68)$$

$$= \pi Q - 2\pi\Lambda + \pi \frac{4\Lambda^2 - Q^2 + 4\alpha^2}{2Q} \ln \left( \frac{\alpha^2 + \Lambda^2 - Q^2/4}{\alpha^2 + (\Lambda - Q/2)^2} \right) + 4\pi\Lambda - 2\pi Q - 4\pi \arctan \left( \frac{\Lambda - Q/2}{\alpha} \right), \quad (69)$$

$$\approx -4\pi \arctan \left( \frac{\Lambda - Q/2}{\alpha} \right) + 4\pi(\Lambda - Q/2) + \frac{\pi Q}{\alpha^2 + \Lambda^2} (\Lambda - Q/2)^2 + \dots, \quad (70)$$

where the expansion on the last line is valid as long as  $Q^2 \ll 4\alpha^2 + 4\Lambda^2$ . This is a reasonable approximation, since  $Q < 2\Lambda$  always, and  $\alpha \gg \Lambda$  usually holds. The expression for the binding energy corresponding to (37) then becomes

$$\alpha \arctan \left( \frac{\Lambda - Q/2}{\alpha} \right) \approx \left[ \frac{m}{2\pi^2 \hbar^2} \left( U_{aa} + \frac{g^2/2}{-\hbar^2 \alpha^2 / m - \varepsilon} \right) \right]^{-1} + (\Lambda - Q/2) \left( 1 + \frac{Q(\Lambda - Q/2)}{4(\alpha^2 + \Lambda^2)} \right). \quad (71)$$

The assumed condition  $Q^2 \ll 4\alpha^2 + 4\Lambda^2$  means that the final term on the right hand side is very little different from  $\Lambda - Q/2$ , so that the effect of non-zero  $Q$  is to replace  $\Lambda$  in the binding energy condition (37) by  $\Lambda - Q/2 < \Lambda$ . This reduction of  $\Lambda$  will have very little effect on the binding energy, as can be seen in Fig. 4.



## References

- [1] P. B. Blakie, A. S. Bradley, M. J. Davis, R. J. Ballagh, and C. W. Gardiner. Dynamics and statistical mechanics of ultra-cold Bose gases using c-field techniques. *Advances in Physics*, 57:363–455, September 2008.
- [2] A. A. Norrie, R. J. Ballagh, and C. W. Gardiner. Quantum turbulence in condensate collisions: an application of the classical field method. *Phys. Rev. Lett.*, 94:040401, 2005.
- [3] A. A. Norrie, R. J. Ballagh, C. W. Gardiner, and A. S. Bradley. Three-body recombination of ultracold Bose gases using the truncated Wigner method. *Phys. Rev. A*, 73(4):043618, Apr 2006.
- [4] A. A. Norrie, R. J. Ballagh, and C. W. Gardiner. Quantum turbulence and correlations in Bose-Einstein condensate collisions. *Phys. Rev. A*, 73(4):043617, Apr 2006.
- [5] E. Braaten and A. Nieto. Quantum Corrections to the Ground State of a Trapped Bose-Einstein Condensate. *Phys. Rev. B*, 56(22):14745–14765, 2006.
- [6] D. J. Heinzen, Roahn Wynar, P. D. Drummond, and K. V. Kheruntsyan. Superchemistry: Dynamics of Coupled Atomic and Molecular Bose-Einstein Condensates. *Phys. Rev. Lett.*, 84(22):5029–5033, May 2000.
- [7] M. Holland, J. Park, and R. Walser. Formation of Pairing Fields in Resonantly Coupled Atomic and Molecular Bose-Einstein Condensates. *Phys. Rev. Lett.*, 86(10):1915–1918, Mar 2001.
- [8] C. E. Sahlberg and C. W. Gardiner. C-Field Method for Ultracold Atom-Molecule Systems II: Stationary Solutions and Bogoliubov Excitations in Atom-Molecule Systems. 2011.
- [9] C. E. Sahlberg, R. J. Ballagh, and C. W. Gardiner. C-Field Method for Ultracold Atom-Molecule Systems III: Dynamic Effects of a Feshbach Resonance on Bragg Scattering from a Bose-Einstein Condensate. 2011.
- [10] S. B. Papp, J. M. Pino, R. J. Wild, S. Ronen, C. E. Wieman, D. S. Jin, and E. A. Cornell. Bragg Spectroscopy of a Strongly Interacting  $^{85}\text{Rb}$  Bose-Einstein Condensate. *Phys. Rev. Lett.*, 101(13):135301, Sep 2008.
- [11] G. Breit. The scattering of slow neutrons by bound protons I. Methods of calculation. *Phys. Rev.*, 71:215, 1947.
- [12] J. M. Blatt and V. F. Weisskopf. *Theoretical nuclear physics*. Wiley, New York, 1952.
- [13] Kerson Huang and C. N. Yang. Quantum-mechanical many-body problem with hard-sphere interaction. *Phys. Rev.*, 105:767, 1957.
- [14] P. D. Drummond, K. V. Kheruntsyan, and H. He. Coherent Molecular Solitons in Bose-Einstein Condensates. *Phys. Rev. Lett.*, 81(15):3055–3058, Oct 1998.
- [15] E. Timmermans, P. Tommasini, M. Hussein, and A. Kerman. Feshbach resonances in atomic Bose-Einstein condensates. *Phys. Rep.*, 315:199–230, 1999.
- [16] R. A. Duine and H. T. C. Stoof. Dynamics of a Bose-Einstein condensate near a Feshbach resonance. *Phys. Rev. A*, 68(1):013602, Jul 2003.
- [17] Yoshio Yamaguchi. Two-Nucleon Problem When the Potential Is Nonlocal but Separable. I. *Phys. Rev.*, 95(6):1628–1634, Sep 1954.

- [18] N. R. Claussen, S. J. J. M. F. Kokkelmans, S. T. Thompson, E. Donley, E. Hodby, and C. E. Weiman. Very-high-precision bound-state spectroscopy near a  $^{85}\text{Rb}$  Feshbach resonance. *Phys. Rev. A*, 67(0):069791, 2003.